Environ Model Assess (2010) 15:397–410
DOI 10.1007/s10666-009-9217-3

A Comprehensive Numerical Model Simulating Gas, Heat, and Moisture Transport in Sanitary Landfills and Methane Oxidation in Final Covers

Anurag Garg · Gopal Achari

Received: 6 June 2008 / Accepted: 11 December 2009 / Published online: 13 January 2010

Abstract A model to simulate gas, heat, and moisture transport through a sanitary landfill has been developed. The model not only considers the different processes that go on in a landfill but also the oxidation of methane in the final cover. The model was calibrated using published results and field data from a pilot scale landfill in Calgary. The model captures the physics of the different processes quite well. Simulations from the model show that waste permeability had a significant impact on the temperature, pressure distribution, and flux from a landfill. The presence of the final and intermediate covers enhanced the gas storage capacity of the landfill. Biodegradation of the waste was enhanced as the final cover minimized the atmospheric influences. In addition, the composition of landfill gas emitted to the atmosphere was significantly different from the composition of gas generated in landfill due to the presence of covers as some of the methane is oxidized to carbon dioxide. There was no significant benefit of using a final cover of higher depth. The presence and number of intermediate covers had an impact on gas flux and temperature distribution within a landfill.

Keywords Landfill gas · Landfill modeling · LFG generation · LFG transport

A. Garg
Schulich School of Engineering, University of Calgary,
2500 University Drive NW,
Calgary AB T2N 1N4, Canada

G. Achari (✉)
Department of Civil Engineering, University of Calgary,
2500 University Drive NW,
Calgary AB T2N 1N4, Canada
e-mail: gachari@ucalgary.ca

1 Introduction

Waste interaction with moisture, degradation which turns from aerobic to anaerobic as oxygen is consumed, spatial and temporal variations in waste types and in leachate and gas generation, changing biochemistry, varying waste composition with different degradation rates, and presence of daily and intermediate covers are some of the factors that make landfills an extremely complex environment. The intricacies of the different interactive processes combined with the complex environment gives rise to the inherent heterogeneous nature of landfills. These complexities and heterogeneities make mathematical simulation of landfills very difficult and is perhaps the reason why much of landfill-related research is experimental. In this paper, we investigate landfill gas generation and transport by developing, calibrating, and validating a comprehensive numerical model. The model is a step towards simulating the complex landfill environment in the computer which can be used to investigate the impact of different scenarios on gas generation and transport.

Several models for gas flow in landfills have been developed by different researchers over the years. These include, among others, the one-dimensional radial flow model of Lu and Kunz [25]; the one-dimensional model of Findikakis and Leckie [16] for vertical flow of a mixture of methane, carbon dioxide, and nitrogen through sanitary landfills; the enhancement of this model of El-Fadel et al. [14, 15] to include heat generation and transport within landfills; the numerical model of Chen et al. [8, 9] for landfills with passive vent; the two-dimensional analytical model of Young [53, 54] for single-specie gas flow inside a non-isotropic porous medium; the three-dimensional model of Arigala et al. [2], an extension of Young's model, which allowed for both horizontal and vertical orientation of

wells. In addition, Metcalfe and Farquhar [26] proposed a two-dimensional advection–dispersion model, and Nastev [28] developed a gas heat and moisture transport model, which considered three gas components: methane, carbon dioxide, and air. Thomas and Ferguson [43] developed a heat and mass transfer model for an unsaturated porous medium, and Hashemi et al. [20] developed a quasi steady-state three-dimensional model for gas generation and transport in landfills. The model considered a mixture of four-component (CH_4, CO_2, N_2, and O_2) gas and took into account the presence of gas extraction wells. Townsend et al. [44] presented a steady-state one-dimensional analytical landfill gas model for horizontal gas collection system. The simulations were conducted for varying operating conditions such as given fluxes or pressures at upper and lower boundaries. Copty et al. [12] proposed a three-dimensional stochastic model for the generation and transport of landfill gas. Garg and Achari [17] developed a model based on fuzzy logic approach to estimate flow of methane at a sanitary landfill. The model gives an estimate of methane flow considering uncertainties in landfill but does not include information about actual physics.

While a number of models have been developed, none consider the effect of temperature changes on gas generation rate, which was identified as the source of highest uncertainty [12]. Further, these models do not consider methane movement and its oxidation in the final cover, although there are models developed independently for this purpose [33, 34, 42]. Methane oxidation in covers can range between 10% and 70% of methane generated in a landfill [11, 23, 30, 51].

In this paper, a model that incorporates four-component (methane, carbon dioxide, oxygen, and nitrogen) gas and moisture flow through the waste and covers coupled with temperature effects has been developed. The model considers variability in gas and heat generation with depth due to aging of waste as well as the effect of temperature variation on gas generation and transport properties of fluids and thermodynamic properties of solids and fluids in the landfill. In addition, it considers methane oxidation in landfill covers and heat generation in this reaction.

2 Conceptual Model

Due to generation of methane and carbon dioxide in landfills, the pressure within a landfill is higher than atmospheric. The pressure gradient forces these gases and residual air present in the pores towards the atmosphere. In addition, the concentration gradient results in diffusive flow in landfills. While the diffusion of methane and carbon dioxide is outward, oxygen tends to diffuse inward. The upward advective flow of gases is a function of air permeability of porous media, which in turn is affected by the resident moisture content and its downward flow through the media. Infiltration of precipitation results in an increase in the moisture content.

Since the processes of gas generation within landfills are exothermic, the temperature in landfills is generally higher than the ambient temperature. The heat transfer in landfills is governed by convection and conduction. The gas generation process accelerates with increasing temperature and thus is affected as heat is transported across in landfills. Migrating moisture downward carries the heat to the bottom of the landfill, whereas the generated gases tend to carry it upward. As the methane generated in the landfill moves through the final cover, methanotrophic bacteria indigenous to the soil oxidize some of escaping methane into carbon dioxide. Thus, the composition of the gas emitted from the surface is different from the composition in the waste pores.

3 Theoretical Formulations

3.1 Gas Generation and Transport

Transport of each species in the gaseous mixture can be described by following advection–dispersion–reaction equation [3].

$$\varphi \frac{\partial C_i}{\partial t} = -\nabla \left(v_g C_i \right) + \nabla \bullet \left(D_i^s \nabla C_i \right) + G_i \pm R_i \tag{1}$$

Where φ is air-filled porosity of the waste (cubic meters of air-filled voids/ cubic meters of waste), C_i is concentration of the ith component (mol/m^3), v_g is Darcy's velocity of gas phase (m/s), t is time (s), D_i^s is diffusion coefficient of species i in porous medium (m^2/s), G_i is the generation rate for species i (mol/(m^3 s)), and R_i is the reaction rate of gas i (mol/(m^3 s)).

The Darcy velocity v_g can be determined from:

$$v_g = -k_{rg} \frac{k_i}{\mu_m} \left(\nabla P_g - \rho_g g \right) \tag{2}$$

Where, k_i is the permeability of porous media (m^2), k_{rg} is the gas phase relative permeability (dimensionless; see Eq. 28, later), μ_m is dynamic viscosity of gas mixture (Pa s), P_g is gas phase pressure (Pa), ρ_g is the density of gas mixture (kg/m^3), and g is acceleration due to gravity (m/s^2).

The pressure exerted by a mixture of m gases is given by Dalton's law:

$$P_g = \sum_{i=1}^{m} P_i \tag{3}$$

Where P_i represents the pressure exerted by gas component i. Assuming that gases follow ideal gas law, the pressure P_i can be calculated by using:

$$P_i = RC_iT \tag{4}$$

Where R is the universal gas constant (=8.314 J/mol K) and T is the absolute temperature of gas mixture (K). The partial pressure of water in gas phase is considered equal to the saturated water vapor pressure at a given temperature.

The viscosity of a mixture of m gases can be determined by the Wilke method using Eqs. 5 and 6 [40].

$$\mu_m = \sum_{i=1}^{m} \frac{y_i\,\mu_i}{\sum_{j=1}^{m} y_j\,\theta_{ij}} \tag{5}$$

$$\theta_{ij} = \frac{\left\{1 + \left(\frac{\mu_i}{\mu_j}\right)^{1/2}\left(\frac{M_j}{M_i}\right)^{1/4}\right\}^2}{\sqrt{8}\left(1 + \frac{M_i}{M_j}\right)^{1/2}} \tag{6}$$

Where, μ_m is the viscosity of gas mixture (Pa s), μ_i is viscosity of mixture component i (Pa s), y_i and y_j are mole fractions of gas i and j, respectively, M_i and M_j are molecular weights of gas i and j, respectively (kg/mol). The mole fraction of gas i can be calculated as:

$$y_i = \frac{C_i}{\sum_{j=1}^{m} C_j} \tag{7}$$

Viscosity of gas i at varying temperatures can be estimated using Eqs. 8 and 9 [11]:

$$\mu_i = \left(4.0785 \times 10^{-6}\right)\frac{\left(M_iT\right)^{1/2}}{V_{c,i}^{2/3}\,\Omega^*}F_c \tag{8}$$

$$F_c = 1 - 0.2756\,\omega_i \tag{9}$$

Where, $V_{c,i}$ is critical volume of gas i (m^3/mol), ω_i is the acentric factor for gas i [37]. Ω^* is reduced collision integral; reduced collision integral can be calculated using Eq. 10 [29]:

$$\Omega^* = \left(\frac{\beta_1}{T_i^{*\beta 2}}\right) + \frac{\beta_3}{\exp\left(\beta_4 T_i^*\right)} + \frac{\beta_5}{\exp\left(\beta_6 T_i^*\right)} + \beta_7 T_i^{*\beta 2}\sin\left(\beta_8 T_i^{*\beta 9} - \beta_{10}\right) \tag{10}$$

Where, β_1=1.16145, β_2=0.14874, β_3=0.52487, β_4=0.7732, β_5=2.16178, β_6=2.43787, β_7=−6.435×10^{-4}, β_8=18.0323, β_9=−0.76830, β_{10}=7.27371. T_i^* is dimensionless temperature of gas i which is related to potential energy parameter and Boltzman's constant, and it can be calculated using Eq. 11 [11, 29]:

$$T_i^* = \frac{T}{T_{c,i}}x1.2593 \tag{11}$$

Where, $T_{c,i}$ = critical temperature (K) of gas i [37].

The air diffusion coefficient D_i^a (m^2/s) of gas i in a mixture of m gases is given by Eq. 12 [40].

$$D_i^a = \frac{1 - y_i}{\sum_{\substack{j=1 \\ j\neq i}}^{m} \frac{y_j}{D_{ij}}} \tag{12}$$

Where, D_{ij} is the diffusion coefficient of gas i in a binary mixture of gases i and j (m^2/s), which can be determined using following equation [7]:

$$D_{ij} = \frac{0.0149 \times 10^{-4}T^{1.81}\left(\frac{1}{M_i} + \frac{1}{M_j}\right)^{0.5}}{P\left(T_{c,i}T_{c,j}\right)^{0.1405}\left(V_{c,i}^{0.4} + V_{c,j}^{0.4}\right)^2} \tag{13}$$

The diffusion coefficient of a gas i in porous medium is different from the air diffusion coefficient. The ratio of the porous medium diffusion coefficient and the air diffusion coefficient is known as the relative diffusion coefficient. It can be determined using the following empirical relationship [45]:

$$\frac{D_i^s}{D_i^a} = \left[\frac{\varphi - c}{1 - c}\right]^d \tag{14}$$

Where, c and d are constants that depend on the porous medium characteristics. Troeh et al. [45] provides values of these constants for different porous media. The rate of gas generation based on first-order reaction kinetics can be determined using:

$$G_{m,i} = L_0\sum_{j=1}^{n} A_jk_je^{-k_jt_r} \tag{15}$$

Where, k_j is the first-order methane generation rate constant for component j of waste (s^{-1}), $G_{m,i}$ is the generation rate of gas i (m^3/(kg s)), L_0 is ultimate gas generation potential of the waste (m^3/kg), A_j is the fraction of component j in waste mass, and t_r is the age of a waste sub-mass. Eq. 15 is applicable for methane and carbon dioxide since these two gases are generated in the landfill under anaerobic conditions. The fraction of water vapor in the gas phase is

computed based on maximum saturation vapor pressure at a given temperature. Since it takes a long time to fill a landfill, the age of different waste masses are higher at greater depths. As the gas generation peaks at the initial stages of anaerobic conditions, the gas generation rate generally decreases with depth. Assuming the landfill is filled at a constant rate, the age of waste (t_r) can be expressed using a linear expression, given as [2]:

$$t_r = t_0 + t_f\left(\frac{Z}{D}\right) \tag{16}$$

Where, t_0 is the time since closure of the landfill, t_f is the total time to fill the landfill, Z is the depth of waste mass measured from surface, and D is the total depth of the landfill. As the temperature in a landfill changes with heat release due to gas generation, the rate of gas generation also changes. Palmisano and Barlaz [31] observed that rate of gas generation doubles for every 10°C rise in temperature, therefore:

$$\left.\frac{dL}{dt}\right|_{T1+10} = 2 \times \left.\frac{dL}{dt}\right|_{T1} \tag{17}$$

thus, $k_{T1+10}=2k_{T1}$

This can also be represented by:

$$k_{T2} = k_{T1}(1.0718)^{(T2-T1)} \tag{18}$$

3.2 Methane Oxidation in Landfill Cover

For serine pathway, the biochemical methane oxidation can be represented by following equation [47]:

$$38.25CH_4 + 3NH_3 + 63.75O_2 \rightarrow 3C_4H_8O_2N + 26.25CO_2 + 69H_2O \tag{19}$$

For each mole of methane oxidized to carbon dioxide, 632 kJ of heat is generated [21, 52]. The rate of oxidation of methane (R_{CH4}), by assuming double Monod kinetics, is determined by [10]:

$$R_{CH_4} = -\nu_{max}\left[\frac{C_{O_2}}{(K_{O_2}+C_{O_2})}\right]\left[\frac{C_{CH_4}}{(K_{CH_4}+C_{CH_4})}\right]X \tag{20}$$

Where, ν_{max} = maximum methane oxidation rate per unit mass of microorganism (mol/(kg s)), X = density of methanotrophic bacteria (kg/m^3), K_{O2}, K_{CH4} = Monod constants for oxygen and methane (mol/m^3), respectively. The Monod constants are assumed as K_{O2}=0.44 mol/m^3, K_{CH4}=0.05 mol/m^3 [34, 50]. According to Eq. 19, 63.75 mol of oxygen (2.04 kg) are utilized to oxidize 38.25 mol of methane (0.612 kg) while generating 26.25 mol of carbon dioxide (1.155 kg). Thus, the carbon dioxide generation rate and oxygen consumption rate are given as [34]:

$$R_{CO_2} = -0.7R_{CH_4} \tag{21}$$

$$R_{O_2} = 1.7R_{CH_4} \tag{22}$$

3.3 Moisture Transport in Landfills

Water percolating through the waste affects the degree of saturation and the distribution of leachate and gases in the pore spaces, thus lowering the effective permeability of porous media for both phases as well as the heat conductivity [27, 49]. In addition, as the movement of the moisture is primarily in the downward direction, heat is carried in that direction. The flow of moisture in the unsaturated media was modeled after Richard's equation: [3, 4]:

$$C\frac{\partial P_l}{\partial t} = -\nabla\bullet\left(-k_{rl}\frac{k_i}{\mu_l}(\nabla P_l + \rho_l g)\right) \tag{23}$$

Where, k_{rl} is the liquid phase relative permeability (dimensionless), μ_l is the dynamic viscosity of liquid phase (Pa s), the viscosity of water at different temperatures, P_l is pressure of the liquid phase (Pa), ρ_l is density of the liquid phase (kg/m^3), and C is the specific moisture capacity (Pa^{-1}) given by [48]:

$$C = \frac{d\theta}{dP_c} = \frac{-\alpha m}{(1-m)}(\theta_s-\theta_r)S_e^{1/m}\left(1-S_e^{1/m}\right)^m \tag{24}$$

P_c is the capillary pressure (Pa), θ is the volumetric moisture content (volume of moisture/total volume of soil), θ_s and θ_r are saturated and residual volumetric moisture contents, respectively (dimensionless), α (Pa^{-1}), n and m are the Van Genuchten fitting parameters, and S_e is called the effective degree of saturation (dimensionless), and it is given as:

$$S_e = \frac{\theta-\theta_r}{\theta_s-\theta_r} \tag{25}$$

The capillary pressure and relative permeability of liquid phase are related to the effective degree of saturation by the following equations [48]:

$$P_c = \frac{1}{\alpha}\left(S_e^{-1/m}-1\right)^{1/n} \tag{26}$$

$$k_{rl} = \sqrt{S_e}\left[1-\left(1-S_e^{1/m}\right)^m\right]^2 \tag{27}$$

A similar equation for relative permeability of gas phase is given as [32]:

$$k_{rg} = \sqrt{1 - S_e}\left[1 - S_e^{1/m}\right]^{2m} \quad (28)$$

The liquid phase velocity is given by Darcy's law as:

$$v_l = -k_{rl}\frac{k_i}{\mu_l}(\nabla P_l + \rho_l g) \quad (29)$$

3.4 Heat Generation and Transport

Heat is generated in the landfill waste mass due to anaerobic decomposition and in the landfill cover due to exothermic methane oxidation reaction. Heat transfer takes place by conduction in solid phase and by convection in gas and liquid phases. The heat balance equation is written as [15, 22]:

$$\frac{\partial(\rho C_p T)}{\partial t} = \nabla \bullet \left(\kappa \nabla T - \rho_g C_{p,g} v_g T - \rho_l C_{p,l} v_l T\right) + Q_h \quad (30)$$

Where ρ is the average waste density (kg/m^3), C_p is the mass fraction weighted average heat capacity of the porous media (J/(kg K)), ρ_g and ρ_l are gas phase and liquid phase densities (kg/m^3), $C_{p,g}$ and $C_{p,l}$ are constant pressure-specific heat capacities of the gas phase and liquid phase, respectively (J/(kg K)), κ is effective thermal conductivity of porous medium (W/(m K)), and Q_h is the rate of heat generation (J/(m^3 day)). If λ_1 Joules of heat is generated by 1 mol of methane generation and λ_2 Joules of heat is generated by 1 mol of methane oxidation, then the rate of heat generation in waste and cover can be given by following equations:

$$Q_{h,waste} = \lambda_1 G_{CH_4} \quad (31)$$

$$Q_{h,cover} = \lambda_2 R_{CH_4} \quad (32)$$

An estimate of the heat generation by the biodegradation of glucose is given by Rees [39] as:

$$1\,\text{kg}\ C_6H_{12}O_6 \rightarrow 0.25\,\text{kg}\ CH_4 + 0.69\,\text{kg}\ CO_2 + 0.056\,\text{kg dry biomass} + 632\,\text{kJ} \quad (33)$$

From Eq. 33, λ_1=40.448 kJ/mol. In addition, as 632 kJ of heat is generated during the oxidation of 1 mol of methane, λ_2=632 kJ/mol [21, 52].

The specific heat capacity of a gas component i can be calculated using the empirical equation given by [37].

$$C_{p,g,i} = \left(a_0 + a_1 T + a_2 T^2 + a_3 T^3 + a_4 T^4\right)\frac{R}{M_i} \quad (34)$$

Where, $C_{p,g,i}$ is the specific heat capacity (J/(mol K)) of gas i. Coefficients a_0, a_1, a_2, a_3, and a_4 were taken from [37], M_i is the molecular weight of gas component i. The specific heat capacities of water were calculated based on internal energy values at different temperatures. Heat capacity of porous media can be calculated using the equation:

$$C_p = \frac{C_s(1-n)\rho_s + C_{p,l} n S_l \rho_l + C_{p,g} n (1 - S_l)\rho_g}{\rho} \quad (35)$$

Here, n represents the total porosity of the porous medium (dimensionless), S_l represents the liquid phase degree of saturation (dimensionless), C_s is the heat capacity of soil solids (J/(kg K)), and ρ_s is the density of soil solids (kg/m^3). Thermal conductivity of the porous medium κ is calculated according to the following equation [38]:

$$\kappa = \kappa_{dry} + S_l\left(\kappa_{wet} - \kappa_{dry}\right) \quad (36)$$

Where, κ_{wet} corresponds to the thermal conductivity of saturated porous media, and κ_{dry} corresponds to the thermal conductivity of dry porous media.

The model was developed and calibrated for one-dimensional simulation because the data were available only for one-dimensional case. COMSOL Multiphysics 3.2, which is a finite element based software, has been used to develop the model and solve the coupled equations.

4 Model Calibration and Validation

4.1 Landfill Waste

The model was first calibrated for landfill waste, using published data from Complexe Environnemental De St.-Michel (CESM) landfill, located in a former limestone rock quarry, on the northern side of Montreal Island [27]. The purpose of the calibration was to determine the constants "c" and "d" for the landfill waste, required in Eq. 14. These values for landfill waste are not available in literature. CESM is the third largest landfill site in North America, which occupies an area of nearly 190 ha, of which 80 ha is used for landfilling operations [27]. The maximum depth at the site is 70 m. The landfilling in the quarry started in 1968. The landfill did not have a surface cover at the time of data collection. There was an existing gas collection system at the landfill. The methane generation rate constant

and the ultimate gas generation potential were evaluated by fitting the gas recovery data to a first order reaction kinetics equation and assuming uniform age of waste in landfill. The value of methane generation rate constant obtained by this was 0.055 year^{-1}. The composition of the gas generated in the landfill averaged approximately 55% (mol/mol) methane and 45% (mol/mol) carbon dioxide [27, 28]. Simulation was conducted for a 40-m deep one-dimensional waste column as this is the average depth of the landfill.

For the simulation, initial and boundary conditions similar to the ones by Nastev [27] were used. The lower boundary was taken as a zero flux boundary for gas transport and a constant temperature of 20°C. Bottom boundary was considered as saturated boundary for moisture transport. The top boundary was considered as constant concentration and constant temperature boundary. Atmospheric pressure was assumed to be 100 kPa, and atmospheric concentrations were taken as 79% nitrogen and 21% oxygen. The constant temperature at the top boundary was assumed to be equal to 6.6°C. A constant water influx of 401.6 mm/year, as computed by Nastev [27, 28] for uncovered waste, was taken at the top boundary. The initial temperature in the landfill was considered as 27°C to account for temperature increase due to aerobic phase, and partial pressures of gases were taken same as those assigned at the top boundary. The age of the refuse was considered the same throughout the landfill, in line with the assumption made by Nastev [27, 28], thus assuming a uniform gas generation rate. Based on a given k and L_0 values, the initial uniform gas generation rate was 288 m^3/year. The input data for the model are given in Table 1.

A 100-year simulation was conducted, and the temperature and pressure curves were plotted to match with Nastev [27, 28] results. Due to higher gas and heat generation in the early phases of anaerobic decomposition, the landfill temperature rose to about 40°C after 10 years, increased further to about 43°C after 20 years, and decreased steadily thereafter. Pressure also rose to more than 3 kPa above atmospheric temperature. Variation in molar fractions of methane at 2-, 10-, and 30-m depths with time also agreed with Nastev's results (Fig. 1). The calibrated value of c is 0.07 and d is 1.6. These values could not be validated as a second set of data was not available for the landfill waste. Also, information on c and d values for landfill waste could not be found in literature. However, results generally agreed with Nastev's results, and these values provided satisfactory results when the simulations were conducted for calibration and validation in the landfill cover.

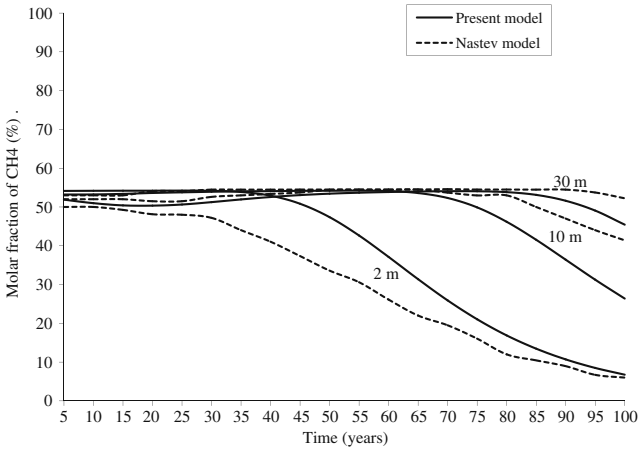

Fig. 1 Variation of molar fraction of methane with time at 2-, 10-, and 30-m depths

Table 1 Input data for CESM landfill

Parameter	Value	Source
Waste depth (m)	40	[27, 28]
Bulk density (kg/m^3)	760	
Particle density (kg/m^3)	1,500	[1]
Total porosity	0.5	[27]
Permeability, k_i (m^2)	1×10^{-12}	[2, 9, 28]
Methane generation rate constant, k (year^{-1})	0.055	[27, 28]
Ultimate methane generation potential, L_0 (m^3/ton)	172	
Total time to fill, t_f (year)	28	[27, 28]
Time since closure, t_0 (year)	0	
vanGenuchten's parameter, m	0.11	[27, 28]
vanGenuchten's parameter, α (Pa^{-1})	5.097×10^{-4}	
Wet heat conductivity, κ_{wet} (W/(m K))	0.184	[27, 28]
Dry heat conductivity, κ_{dry} (W/(m K))	0.038	
Specific heat of waste particles, C_s (J/(kg K))	1,333	
Saturated volumetric moisture content, θ_s	0.5	[27, 28]
Residual volumetric moisture content, θ_r	0.015	

The boundary conditions for the landfill simulation to calibrate the model for landfill waste were taken similar to Nastev's model so that the outputs can be matched and the values of coefficients c and d determined. However, it was realized that a constant temperature boundary condition at the base does not represent a realistic case. The temperature at the bottom boundary is expected to vary with time due to variation in different processes responsible for heat generation and transfer within the landfill. Since the bottom boundary is a zero gas flux boundary, the convective heat flux will also be zero there, while the conductive heat transfer across this boundary can still take place. Therefore, in the rest of the simulations, the bottom boundary condition was modified to a zero convective heat flux condition. This is in line with the zero gas flux boundary condition.

4.2 Landfill Cover

The model was then calibrated to determine the v_{max} for methane oxidation in landfill cover using data reported in Perera [33] from a field test cell in the City of Calgary. The v_{max} value was adjusted to match the measured concentrations in landfill cover and the measured flux on landfill surface at two locations (Locations 1 and 2) in the test cell. Data from Location 1 at test cell was used to calibrate the model. Model was later validated using the data from Location 2.

The test cell which had a top area of 29.5×37 m, a bottom area of 7×7 m, and a maximum depth of 3.75 m with a geomembrane bottom liner placed on top of a 900-mm thick compacted clay liner is described in detail in Perera [33] and Perera et al. [36]. The maximum methane oxidation rate in the landfill cover was found to be 6.5×10^{-8} mol/(kg s). Concentrations of methane, carbon dioxide, oxygen, and nitrogen in landfill cover and surface flux were measured in July 2000, which were used for model calibration. No methane emission was detected in flux measurement while the average carbon dioxide flux was found to be 8 g/(m^2 day). The maximum measured CO_2 flux was 41 g/(m^2 day). The waste and cover data used for model calibration and validation are given in Tables 2 and 3, respectively. The calibrated values of constants c and d for landfill waste as generated in previous section were used for waste in test cell.

In this model, it was assumed that the gas generated in landfill is 50% (mol/mol) methane and 50% (mol/mol) carbon dioxide. To determine the biodegradation rate constant, k, the methodology proposed in Garg et al. [18] was used. The biodegradable fraction of waste was estimated to be about 69% based on data provided in Perera [33]. Based on the data and meteorological information of Perera [33] pertaining to Calgary, a methane generation rate constant value of 0.011 $year^{-1}$ was calculated [18], which is in line with a value of 0.01 $year^{-1}$ used by CH2MHILL [6] for a study of a City of Calgary landfill.

For simulating the test cell, the bottom boundary was considered as a no-flux boundary for gas components. Only conductive heat flux was considered at the bottom boundary. Since a drainage layer was provided at the base of the landfill for leachate collection, it was considered as a

Table 2 Model input data for test cell waste

Parameter	Location 1	Location 2	Source
Waste depth (m)	3	3.75	[33]
Bulk density (kg/m^3)	585	585	[33]
Particle density (kg/m^3)	1,400	1,400	[1]
Total porosity	0.65	0.65	[33]
Permeability, k_i (m^2)	1×10^{-12}	1×10^{-12}	[2, 9]
Methane generation rate constant, k ($year^{-1}$)	0.011	0.011	Calculated
Ultimate methane generation potential, L_0 (m^3/ton)	170	170	[46]
Total time to fill, t_f (year)	0	0	[33]
Time since closure, t_0 (year)	0	0	[33]
vanGenuchten's parameter, m	0.11	0.11	[27]
vanGenuchten's parameter, α (Pa^{-1})	5.097×10^{-4}	5.097×10^{-4}	[27]
Coefficients c, d for relative diffusion	0.07, 1.6	0.07, 1.6	Calibrated values
Wet heat conductivity, κ_{wet} (W/(m K))	0.184	0.184	[27]
Dry heat conductivity, κ_{dry} (W/(m K))	0.038	0.038	[27]
Specific heat of waste particles, C_s (J/(kg K))	1,333	1,333	[27]
Saturated volumetric moisture content, θ_s	0.65	0.65	[27]
Residual volumetric moisture content, θ_r	0.0195	0.0195	[27]

Table 3 Model input data for test cell cover

Parameter	Location 1	Location 2	Source
Cover thickness (m)	0.64	0.66	[33]
Bulk density (kg/m^3)	1,650	1,650	[33]
Particle density (kg/m^3)	2,400	2,400	[33]
Total porosity	0.44	0.44	[33]
Permeability, k_i (m^2)	1×10^{-13}	1×10^{-13}	[33]
vanGenuchten's parameter, m	0.625	0.625	[27]
vanGenuchten's parameter, α (Pa^{-1})	2.69×10^{-6}	2.69×10^{-6}	[27]
Wet heat conductivity, κ_{wet} (W/(m K))	0.828	0.828	[27]
Dry heat conductivity, κ_{dry} (W/(m K))	0.27	0.27	[27]
Specific heat of soil particles, C_s (J/(kg K))	1,380	1,380	[27]
Saturated volumetric moisture content, θ_s	0.33	0.33	Assumed
Residual volumetric moisture content, θ_r	0	0	[27]

sink for moisture transport. The top boundary was considered as the constant concentration and a constant temperature boundary. The concentrations, as measured by Perera [33], were taken at the top boundary. The average daily temperature for Calgary was taken as the constant temperature top boundary. For moisture transport, a constant flux was considered as the top boundary. Twenty percent of the annual precipitation was distributed over a year and was taken as the influx into the test cell. This assumption was evaluated by changing the infiltration to 10% and 30%, and no significant impact was observed on gas concentrations, temperature, and gas flux. Initial concentrations of gas components in landfill were considered as same as the atmospheric concentrations. Initial temperature was assumed to be 286.8 K, same as the average daily temperature for the month of June in which the test cell was constructed.

The concentration of gas components as obtained from the model were compared to measured data for Location 1 (Fig. 2). Model results are generally in agreement with the measured values. The flux value obtained from the model for Location 1 was 0.210 mol/(m^{2}day) compared to a measured value of 0.142 mol/(m^{2}day). The difference is explained by the fact that closed flux chambers were used for measurements, which usually underestimates the flux [35, 41]. The calibrated value of v_{max} for Location 1 is 3.0×10^{-9} mol/kg s.

The model was validated using data from Location 2 at the test cell. Model results along with the measured data at Location 2 are shown in Fig. 3. The v_{max} value obtained in model calibration was used here. Here again, the results generally agree with the measured values. The flux values obtained from the model was 0.352 mol/(m^{2}day) compared to a measured value of 0.326 mol/(m^{2}day).

5 Model Simulation Results

After the model had been satisfactorily calibrated for both the waste and the final cover, simulations were conducted to study the effect of waste permeability, presence of final cover and its thickness, presence of intermediate cover and its thickness, and number of intermediate covers. For the purpose of conducting the simulations, data from CESM

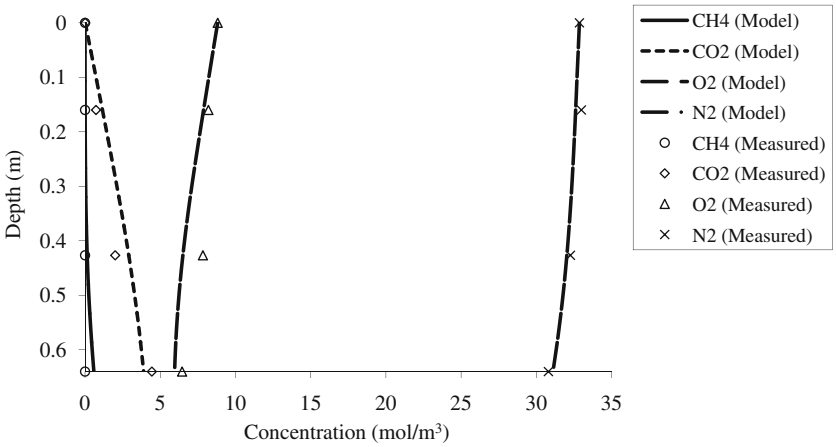

Fig. 2 Variation of concentration with cover depth at Location 1 of test cell: Model calibration

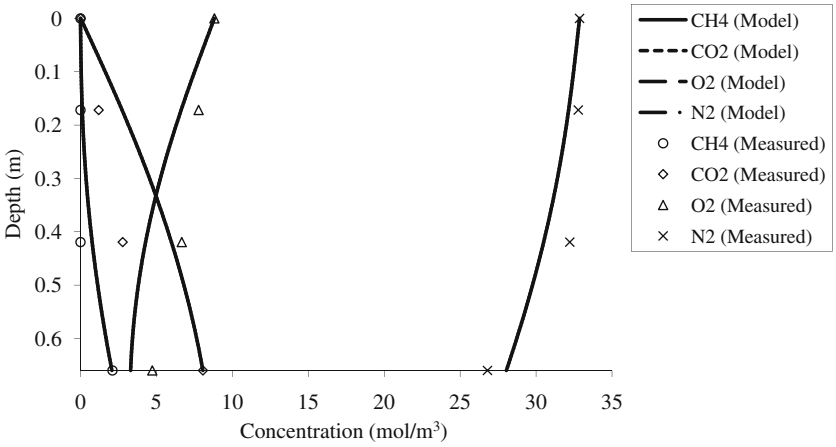

Fig. 3 Variation of concentration with cover depth at Location 2 of test cell: Model validation

landfill were used. Data for final cover were taken from test cell in the City of Calgary.

5.1 Effect of Waste Permeability

Two simulations with waste permeabilities of 1×10^{-12} and $1\times10^{-11}\,m^2$ were conducted to study the effect of waste permeability on gas dynamics in landfill. The temperature and pressure plots for the both simulations are given in Figs. 4 and 5, respectively. As expected, the temperature and pressure plots indicate by increasing the permeability, the gas, and heat loss increased; thus, lower temperature and pressure were obtained from simulation. In both cases, the temperature in the landfill increased even after 10 years in the deeper regions of the landfill. This may be due to the higher heat loss to the atmosphere from the upper regions in the initial years when the rate of biodegradation was higher. The pressure reached a value of only 100.6 kPa as opposed to 101.1 kPa after 10 years in lower waste permeability simulation. This again is on account of increased gas loss to the atmosphere.

The surface gas fluxes over time for the two permeabilities are shown in Fig. 6. The methane flux rate after 5 years increased from 8.5 to 9.05 mol/(m^2day) when the permeability was increased by an order of magnitude. Though higher fluxes for higher waste permeability were observed for initial years, it was lower beyond about 30 years. This is because the gas concentrations were higher in low permeability waste due to lower gas losses in initial years. The total fluxes after 5 years were 14.95 and 14.2 mol/(m^2day), respectively, for higher and lower permeability simulations.

5.2 Effect of Oxidative Final Cover

Simulations were conducted to study the effect of oxidative final cover and its thickness on temperature, pressure, and surface gas flux. Two cases were considered for a landfill with final cover; one with 1-m thickness and the other with 1.5-m thickness. The cover properties were considered the same as for the City of Calgary test cell data used for model calibration (Table 3). A v_{max} of 3×10^{-9}mol/(kg s) as

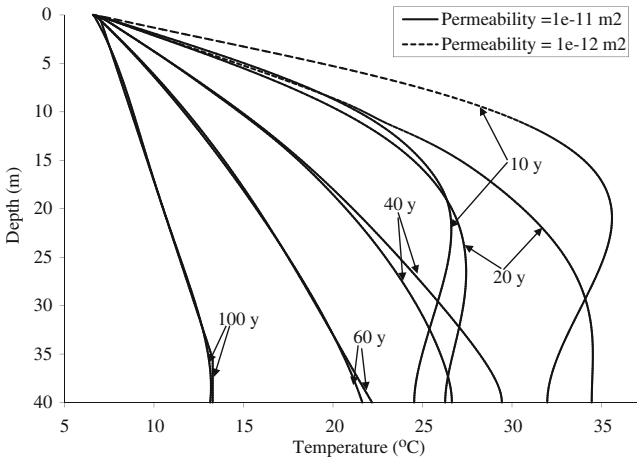

Fig. 4 Temperature plots against time for CESM landfill for simulations conducted with different waste permeabilities

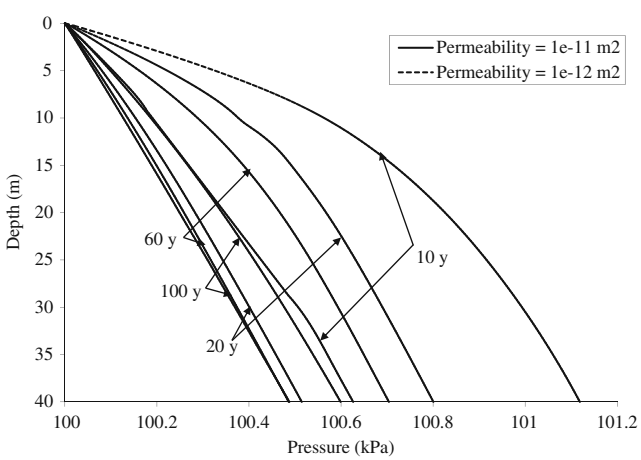

Fig. 5 Impact of waste permeability on pressure distribution with depth for CESM landfill

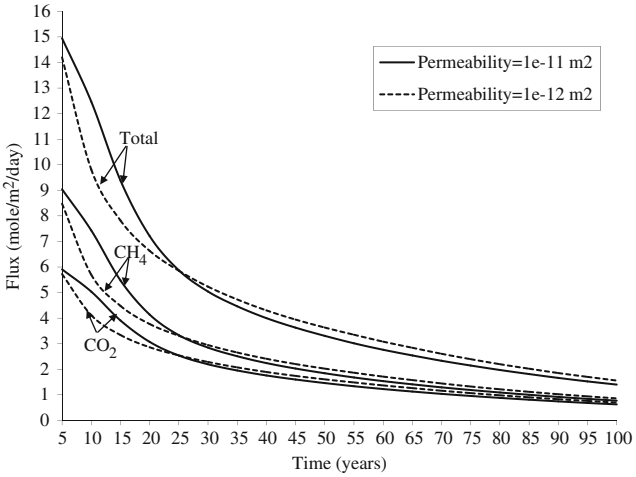

Fig. 6 Surface flux with time for CESM landfill without final cover for waste permeability of 1×10^{-12} and $1\times10^{-11}\,m^2$

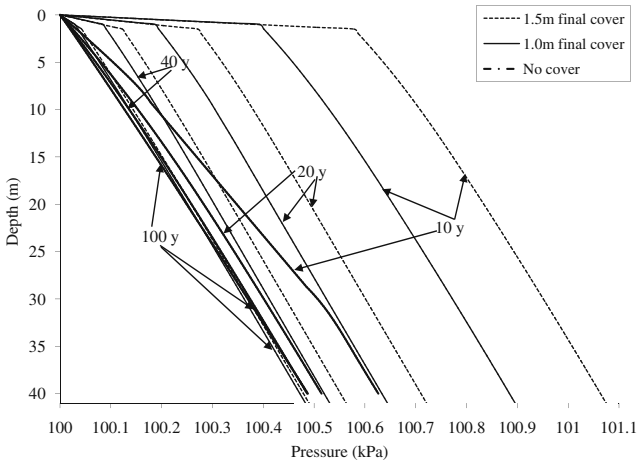

Fig. 8 Comparison of pressure distribution with depth for landfill with 1.5-m oxidative final cover, 1-m oxidative final cover (permeability= $1\times10^{-13}\,m^2$), and a landfill with no final cover

obtained in model calibration was considered. A waste permeability of $1\times10^{-11}\,m^2$ was used in the simulations.

The temperature and pressure plots for landfills with no cover, 1-m cover, and 1.5-m cover are given in Figs. 7 and 8, respectively. The impact of the final cover on temperature distribution in a landfill was significant. Noteworthy difference in temperature distribution between a final cover of 1-m and 1.5-m thickness was not observed. Unlike in the simulations of landfills without final cover, the temperature in the middle to lower parts of landfill with 1-m and 1.5-m cover remained largely in the range of 30–37°C. These are in line with earlier findings that the expected temperature in the anaerobic zone is around 35°C [5, 19, 24]. This shows that the final cover reduces heat loss from the landfill, and additional cover thickness provides limited benefits. When covers were used, the temperatures after 10 years were about 37°C at depths of 12 to 17 m. The pressure rose to about 0.9 and 1.1 kPa above atmospheric pressure at the bottom of landfill in case of 1.0 and 1.5-m final covers, respectively. At lower depths of the landfill, there was more pressure buildup when the landfill had a final cover. The flux plots in Fig. 9 indicate a significant reduction in surface gas flux from the landfill when a final cover is used. The total methane and carbon dioxide flux after 5 years were 12.17 mol/(m^2day) in a landfill with a 1-m cover as compared to 14.95 mol/(m^2day) in an open landfill. The flux rate remained lower for covered landfill until about 60 years. An increase in the cover thickness from 1 to 1.5 m resulted in a reduction of the total methane flux from 7.21 to 5.97 mol/(m^2day) after 5 years. The total flux also reduced from 12.17 to 10.02 mol/(m^2day). The fraction of methane in the emitted gas was reduced due to higher rate of oxidation to carbon dioxide. These results are in line with the findings of Natev et al. [28], who found enhanced

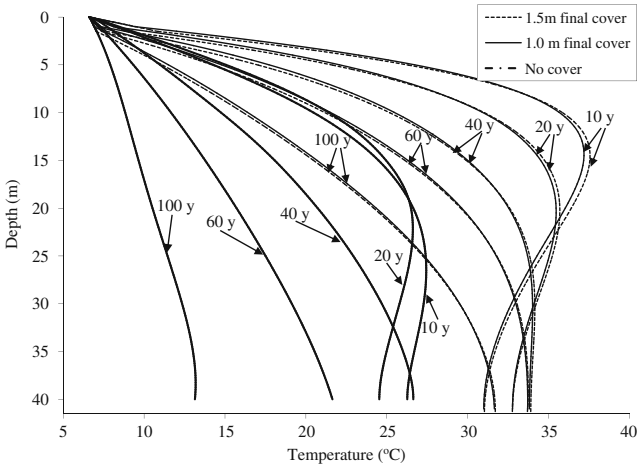

Fig. 7 Comparison of temperature distribution with depth for landfill with 1.5-m oxidative final cover, 1-m oxidative final cover (permeability= $1\times10^{-13}\,m^2$), and a landfill with no final cover

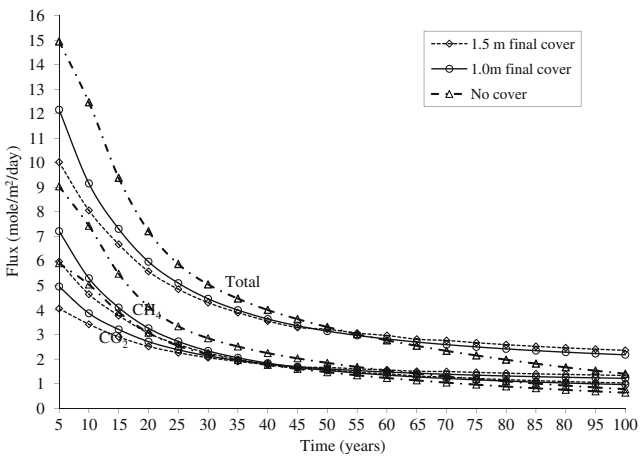

Fig. 9 Methane and carbon dioxide surface fluxes for landfill with 1.5-m final cover, 1.0-m final cover (permeability=$1\times10^{-13}\,m^2$), and no cover

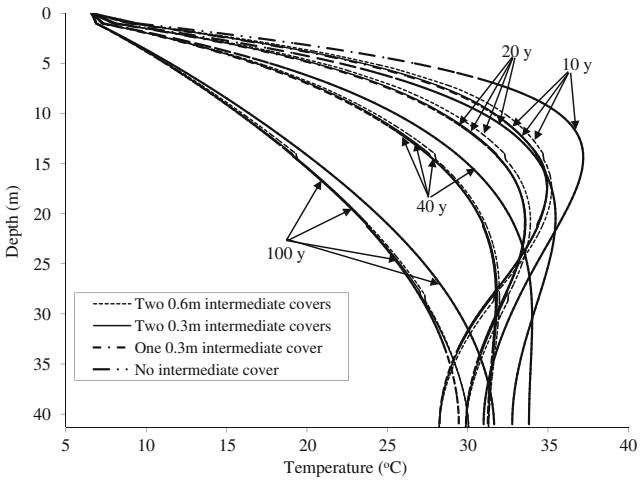

Fig. 10 Temperature distribution with depth for landfill with two 0.3-m thick intermediate covers, one 0.3-m intermediate cover, two 0.6-m intermediate cover, and no intermediate cover (intermediate and final cover permeability=1×10^{-13} m^2)

methane extraction in case of covered landfills due to lower emissions at surface. Also, Nastev et al. [28] observed that due to decreased air intrusion in covered landfills, methane content was higher in recovered gas. Chen et al. [9] also concluded that increasing cover thickness resulted in increased gas recovery in passive vent.

These results indicate that the gas recovery by an extraction system will be higher from a closed landfill. Also, if the gas generation in a landfill is not sufficient to support gas extraction, a final cover with high oxidative properties can help reduce methane emissions from the landfill by oxidizing it to carbon dioxide.

5.3 Impact of Intermediate Covers

Simulations were conducted to study the impact of intermediate covers on gas and heat dynamics in a landfill. One 0.3-m thick intermediate cover, two 0.3-m intermediate covers, and two 0.6-m intermediate covers along with a 1-m thick final cover were simulated. The intermediate cover was placed midway (21 m from surface of final cover) for the single intermediate cover and about one-third way (14 m from surface) and two-thirds way (27.8 m from surface) for the two covers. The total waste column was 40 m. The properties of intermediate cover were assumed to be the same as those of the final cover except that there was no gas generation or oxidation taking place in intermediate covers.

The temperature curves in Fig. 10 show lower temperatures in the landfills with intermediate cover than the landfill without an intermediate cover. The maximum temperature in the landfill after 10 years was about 35°C when it had an intermediate cover. The maximum temperature after 10 years in the landfill without an intermediate cover was about 37°C. This may be because the higher gas and heat generating newer waste in the top portion of the landfill was separated from older waste by the intermediate cover. With intermediate covers, there was more heat transfer in the upper direction from the heat-generating top layer (intermediate covers acting somewhat as a barrier) than the lower direction resulting in a higher net heat loss from the landfill system. This also explains a lower temperature near the bottom in the case of a landfill with intermediate cover than a landfill without an intermediate cover. When two covers were considered, there was no significant difference observed in the temperature profiles. Although the temperature was slightly higher in the case of landfill with two intermediate covers, that difference is not significant. The temperature plots indicate a higher temperature in the case of two 0.6-m intermediate covers. Thus, increasing the intermediate cover thickness resulted in reduced heat loss from the landfill.

The pressure plot in Fig. 11 indicates slightly higher pressure below the intermediate covers. The pressure increase after 10 years near the bottom of landfill with a single intermediate cover was 0.92 kPa above the atmospheric pressure as compared to 0.89 kPa in the case of a landfill without an intermediate cover. The pressure in the landfill with an intermediate cover remained higher for most of the simulated period. In addition, there was a steep pressure drop across the intermediate cover until about 20 years. This pressure difference across the intermediate cover diminished over time and became rather gradual. The pressure was higher in the case of two intermediate covers due to decreased gas loss from the landfill. There was a steep pressure drop across the top intermediate cover until about 40 years, which became rather gradual later on. This steep drop was not perceptible across the lower intermedi-

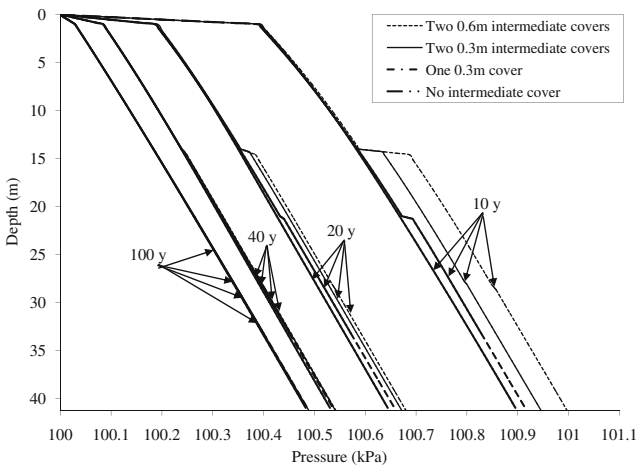

Fig. 11 Pressure distribution with depth for landfill with two 0.3-m thick intermediate covers, one 0.3-m intermediate cover, two 0.6-m intermediate cover, and no intermediate cover (intermediate and final cover permeability 1×10^{-13} m^2)

ate cover. The pressure gradient across the 0.6-m intermediate cover was steeper than the 0.3-m intermediate cover. The pressure near the bottom of landfill with 0.6-m intermediate cover after 10 years was 1.0 kPa above atmospheric pressure compared to 0.95 kPa in the case of 0.3-m intermediate cover.

Variation in flux rate with time is plotted in Fig. 12 for landfills with and without intermediate covers. The initial flux was highest when there was no intermediate cover and lowest when there were two intermediate covers each of 0.6-m thickness. Until about 35 years, the flux rates were lower in the case of a landfill with an intermediate cover than the landfill without an intermediate cover. The total gas flux rates after 5 years were 8.01 mol/(m^2day) in the case of the landfill with a single intermediate cover compared to 12.17 mol/(m^2day) in landfill without an intermediate cover. The total methane and carbon dioxide flux rates in landfill with intermediate cover were more after 35 years than the landfill without an intermediate cover. This is because the concentrations of these gases were more in the landfill with intermediate cover due to lesser losses in previous years.

The gas fluxes at the surface were slightly higher when two intermediate covers were used although this difference was not significant. This higher flux may be due to higher gas loss to the atmosphere from the shallow portions of the landfill generating more gas and separated by a low permeability intermediate cover in the case of two intermediate covers landfill. This indicates that not only the number of covers but also the depth of waste affect the surface flux. The total gas flux rates were 8.16 and 8.02 mol/(m^2day) in the case of two and one intermediate cover landfills, respectively. The plots for surface flux indicate a lower flux when 0.6-m thick intermediate covers were used. This indicates that the gas loss from the waste below the intermediate cover was reduced by increasing the intermediate cover thickness. The methane flux after 5 years was 3.39 mol/(m^2day) in the case of 0.6-m covers as compared to 4.79 mol/(m^2day) in the case of 0.3-m covers.

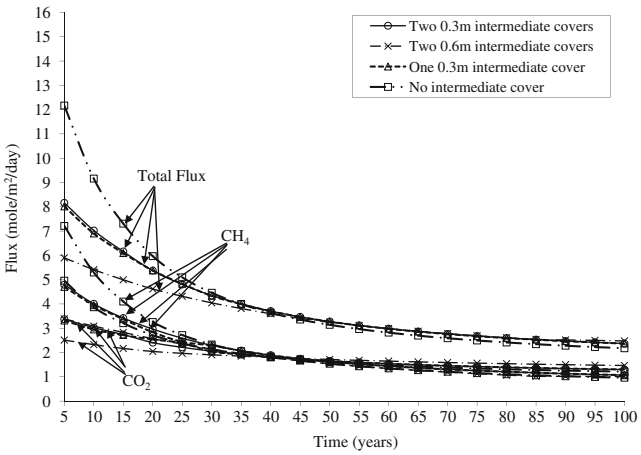

Fig. 12 Methane and carbon dioxide flux for landfill with two 0.3-m thick intermediate covers, one 0.3-m intermediate cover, two 0.6-m intermediate cover, and no intermediate cover (intermediate and final cover permeability 1×10^{-13} m^2)

6 Conclusions

A gas (CH_4 CO_2, O_2, and N_2), heat, and moisture transport model for the landfill was developed to determine the gas and temperature distribution and the surface flux from a landfill. The model considers temperature feedback on the gas generation and the oxidation of methane in the final cover. The effect of moisture on the permeability of the porous media was considered. The model was calibrated using the data from a test cell in The City of Calgary and a landfill in the City of Montreal.

Simulations were conducted to investigate the effect of final cover and its thickness; the presence of intermediate covers, number of intermediate covers, and their thicknesses on gas; and heat dynamics in landfills. Atmospheric interference was reduced significantly by the presence of final cover, which is in line with findings in literature. The presence of the final cover increased the pressure within the landfill. Increasing the cover thickness resulted in further increase in gas pressure. The flux rates were reduced by providing final cover and by further increasing the cover thickness. Due to methane oxidation in the final cover, the carbon dioxide fraction increased in the total emissions when an oxidative final cover was present. However, increasing the cover thickness to 1.5 from 1.0 m did not have a significant impact on carbon dioxide fraction in gas emissions. The presence of intermediate cover also had significant impact on gas and heat dynamics in landfill. The intermediate cover separated the high gas and heat generating waste in top region of landfill from the waste in the deeper regions. This resulted in the higher heat loss from the top region to the atmosphere, and temperatures were slightly lower in the landfill with an intermediate cover. The pressure in the regions below intermediate cover was higher due to reduced gas loss from this part of the landfill. In addition, the surface gas fluxes were reduced in the initial years from the landfill. By providing two intermediate covers, the temperature in landfill increased; however, this difference was not very significant. The pressure in landfill increased further by introduction of second intermediate cover. By increasing the intermediate cover thickness, the temperature in the landfill increased. Also, the pressure increased in the landfill, and the surface gas fluxes decreased by increasing the thickness of intermediate cover. The pressure rise was more below intermediate cover, and in initial years, the pressure

gradient across the intermediate cover was significant. These results indicate that the presence of final cover and intermediate cover can enhance the gas recovery from landfill due to higher pressure within the landfill.

References

1. Agnew, J. M., & Leonard, J. J. (2003). The physical properties of compost. *Compost Science and Utilization, 11*(3), 238–264.
2. Arigala, S. G., Tsotsis, T. T., Webster, I. A., Yortsos, Y. C., & Kattapuram, J. J. (1995). Gas generation, transport and extraction in landfills. *Journal of Environmental Engineering, 121*(1), 33–44.
3. Bear, J. (1972). *Dynamics of fluids in porous media*. New York: Elsevier.
4. Bear, J. (1979). *Hydraulics of groundwater*. London: McGraw-Hill.
5. Bingmer, H. G., & Crutzen, P. J. (1987). The production of methane from solid wastes. *Journal of Geophysical Research, 92* (D2), 2181–2187.
6. CH2MHILL. (2002). *Landfill gas feasibility assessment study for the City of Calgary Solid Waste Services Division*. Calgary: City of Calgary Solid Waste Services Division.
7. Chen, N. H., & Othmer, D. F. (1962). New Generalized equation for gas diffusion coefificient. *Journal of Chemical and Engineering Data, 7*(1), 37–41.
8. Chen, Y.-C., Wu, C.-H., & Hu, H.-Y. (2000). Numerical simulation of gas emission in a sanitary landfill equipped with a passive venting system. *Journal of Environmental Science & Health, A35*(9), 1735–1747.
9. Chen, Y.-C., Chen, K.-S., & Wu, C.-H. (2003). Numerical simulation of gas flow around a passive vent in a sanitary landfill. *Journal of Hazardous Materials, B100, 39–52.*
10. Cherry, R. S., & Thompson, D. N. (1997). Shift from growth to nutrient-limited maintenance kinetics during biofilter acclimation. *Biotechnology and Bioengineering, 56*(3), 330–339.
11. Chung, T.-H., Ajlan, M., Lee, L. L., & Starling, K. E. (1988). Generalized multiparameter correlation for nonpolar and polar fluid transport properties. *Industrial & Engineering Chemistry Research, 27*(4), 671–679.
12. Copty, N. K., Ergene, D., & Onay, T. T. (2004). Stochastic model for landfill gas transport and energy recovery. *Journal of Environmental Engineering, 130*(9), 1042–1049.
13. Czepiel, P. M., Mosher, B., Crill, P. M., & Harriss, R. C. (1996). Quantifying the effect of oxidation on landfill methane emissions. *Journal of Geophysical Research, 101*(D11), 16721–16729.
14. El-Fadel, M., Findikakis, A. N., & Leckie, J. O. (1996). Numerical modelling of generation and transport of gas and heat in sanitary landfills I. Model formulation. *Waste Management & Research, 14*, 483–504.
15. El-Fadel, M., Findikakis, A. N., & Leckie, J. O. (1996). Numerical modelling of generation and transport of gas and heat in sanitary landfills II. Model application. *Waste Management & Research, 14*, 537–551.
16. Findikakis, A. N., & Leckie, J. O. (1979). Numerical simulation of gas flow in Sanitary Landfills. *Journal of Environmental Engineering Division, 105*, 927–945.
17. Garg, A., & Achari, G. (2007). Application of fuzzy logic to estimate flow of methane for energy generation at a sanitary landfill. *Journal of Energy Engineering, 133*(4), 212–223.
18. Garg, A., Achari, G., & Joshi, R. C. (2006). A model to estimate the methane generation rate constant in sanitary landfills using fuzzy synthetic evaluation. *Waste Management & Research, 24* (4), 363–375.
19. Gunnerson, C. G., & Stucky, D. C. (1986). Integrated resource recovery: Anaerobic digestion principles and practices for biogas systems. World Bank technical paper no. 49, UNDP project report no. 5, Washington D.C.
20. Hashemi, M., Kavak, H. I., Tsotsis, T. T., & Sahimi, M. (2002). Computer simulation of gas generation and transport in landfills-I: quasi-steady-state condition. *Chemical Engineering Science, 57*, 2475–2501.
21. Hettiarachchi, V. C. (2005). Mass, heat, and moisture transport in methanobiofilters. Ph.D. thesis, University of Calgary, Calgary, Canada.
22. Kaviany, M. (1995). *Principles of heat transfer in porous media*. New York: Springer.
23. Kightley, D., Nedwell, D. B., & Cooper, M. (1995). Capacity of methane oxidation in landfill cover soils measured in laboratory scale soil microcosms. *Applied and Environmental Microbiology, 61*(2), 592–601.
24. Levelton, B. H., & Associates. (1991). *Inventory of methane emissions from landfills in Canada*. Environment Canada, File 490–974, June 1991, Richmond, B.C.
25. Lu, A.-H., & Kunz, C. O. (1981). Gas flow model to determine methane production at sanitary landfills. *Environmental Science & Technology, 15*(4), 436–440.
26. Metcalfe, D. E., & Farquhar, G. J. (1987). Modelling gas migration through unsaturated soils from waste disposal sites. *Water, Air, and Soil Pollution, 32*, 247–259.
27. Nastev, M. (1998). Modelling landfill gas generation and migration in sanitary landfills and geological formations. Ph.D. dissertation, Laval University, Quebec, Canada.
28. Nastev, M., Therrien, R., Lefebvre, R., & Gelinas, P. (2001). Gas production and migration in landfills and geological materials. *Journal of Contaminant Hydrology, 52*, 187–211.
29. Neufeld, P. D., Janzen, A. R., & Aziz, R. A. (1972). Empirical equation to calculate 16 of the transport collision integrals for the Lennard-Jones (12-6) potential. *Journal of Chemical Physics, 57* (3), 1100–1102.
30. Nozhevnikova, A. N., Nekrasova, V. K., Lebedev, V. S., & Lifshits, A. B. (1993). Microbiological processes in landfills. *Water Science Technology, 27*, 243–252.
31. Palmisano, A. C., & Barlaz, M. A. (1996). *Microbiology of solid waste*. New York: CRC.
32. Parker, J. C. (1989). Multiphase flow and transport in porous media. *Review of Geophysics, 27*(3), 311–328.
33. Perera, L. A. K. (2001). Gas migration model for sanitary landfill cover systems. Ph.D. Thesis, University of Calgary, Calgary.
34. Perera, L. A. K., Achari, G., & Hettiaratchi, J. P. A. (2002). Determination of source strength of landfill gas: a numerical modeling approach. *Journal of Environmental Engineering, 128* (5), 461–471.
35. Perera, M. D. N., Hettiaratchi, J. P. A., & Achari, G. (2002). A mathematical modeling approach to improve the point estimation of landfill gas surface emissions using the flux chamber technique. *Journal of Environmental Engineering and Science, 1*, 451–463.
36. Perera, L. A. K., Achari, G., & Hettiaratchi, J. P. A. (2004). An assessment of the spatial variability of greenhouse gas emissions from landfills: a GIS based statistical-numerical approach. *Journal of Environmental Informatics, 4*(1), 11–30.
37. Poling, B. E., Prausnitz, J. M., & O'Connell, J. P. (2001). *The properties of gases and liquids*. New York: McGraw-Hill.
38. Pruess, K. (1991). *TOUGH 2—a general purpose numerical simulator for multiphase fluid and heat flow*. Berkeley: Earth Science Division, Lawrence Berkley Laboratory, University of California.
39. Rees, J. F. (1980). The fate of carbon compounds in the landfill disposal of organic matter. *Journal of Chemical Technology and Biotechnology, 30*, 161–175.

40. Reid, R. C., Prausnitz, J. M., & Poling, B. E. (1987). *The properties of gases and liquids*. New York: McGraw-Hill.
41. Senevirathna, D. G. M., Achari, G., & Hettiaratchi, J. P. A. (2006). A laboratory evaluation of errors associated with the determination of landfill gas emissions. *Canadian Journal of Civil Engineering, 33*, 240–244.
42. Stein, V. B., Hettiaratchi, J. P. A., & Achari, G. (2001). A numerical model for biological oxidation and migration of methane in soils. *Practice Periodical of Hazardous, Toxic and Radiative Waste Management, 5*(4), 225–234.
43. Thomas, H. R., & Ferguson, W. J. (1999). A fully coupled heat and mass transfer model incorporating contaminant gas transfer in an unsaturated porous medium. *Computers and Geotechnics, 24*, 65–87.
44. Townsend, T. G., Wise, W. R., & Jain, P. (2005). One-dimensional gas flow model for horizontal gas collection systems at municipal solid waste landfills. *Journal of Environmental Engineering, 131* (12), 1716–1723.
45. Troeh, F. R., Jabro, J. D., & Kirkham, D. (1982). Gaseous diffusion equations for porous materials. *Geoderma, 27*, 239–253.
46. USEPA (2005). Landfill Gas Emissions Model (LandGEM) Version 3.02 User's Guide, EPA-600/R-05/047 http://www.epa.gov/ttn/catc/products.html#software.
47. Van Dijken, J. P., & Harder, W. (1975). Growth yields of microorganisms on methanol and methane. A theoretical study. *Biotechnology and Bioengineering, 17*(1), 15–30.
48. Van Genuchten, M. T. (1980). A closed form equation for predicting the hydraulic conductivity of unsaturated soils. *Soil Science Society of America Journal, 44*, 892–898.
49. Vigneault, H., Lefebvre, R., & Nastev, M. (2004). Numerical simulation of the radius of influence for landfill gas well. *Vadose Zone Journal, 3*, 909–916.
50. Visscher, A. D., Thomas, D., Boeckx, P., & Cleemput, O. V. (1999). Methane oxidation in simulated landfill cover soil environments. *Environmental Science & Technology, 33*(11), 1854–1859.
51. Whalen, S. C., Reebugh, W. S., & Sandberk, K. A. (1990). Rapid methane oxidation in landfill cover soil. *Applied and Environmental Microbiology, 56*(11), 3405–3411.
52. Wilshusen, J. H. (2003). An investigation of the role of oxygen and nitrogen in methane oxidation and the formation of exopolymeric substances (EPS) in biofilters. Masters Thesis, University of Calgary, Calgary.
53. Young, A. (1989). Mathematical modelling of landfill degradation. *Journal of Chemical Technology and Biotechnology, 46*, 189–208.
54. Young, A. (1989). Mathematical modelling of landfill gas extraction. *Journal of Environmental Engineering, 115*(6), 1073–1087.